



OPEN ACCESS

EDITED BY

Hualin Zhang,
University of Southern California, United States

REVIEWED BY

Sina Mossahebi,
University of Maryland, United States
Zhong Su,
McLaren Regional Medical Center,
United States

*CORRESPONDENCE

Joshua S. Niedzielski
✉ jsniedzielski@mdanderson.org
Yuting Li
✉ YLi30@mdanderson.org

RECEIVED 23 October 2025

REVISED 18 December 2025

ACCEPTED 30 December 2025

PUBLISHED 04 February 2026

CITATION

Li Y, Martin-Paulpeter RM, Chung CV, Aguilar MA, Matias CA, Delgado A, Nair SS, Court LE, Perles L, Sahoo N, Zhu RX, Poenisch F, Flint DB, Sawakuchi GO, Beddar S, Koay E, Baker JS, Ludmir EB and Niedzielski JS (2026) Novel pencil-beam scanning proton lattice radiation therapy for the treatment of bulky liver cancer: dosimetric comparison with VMAT-lattice radiotherapy.
Front. Oncol. 15:1731259.
doi: 10.3389/fonc.2025.1731259

COPYRIGHT

© 2026 Li, Martin-Paulpeter, Chung, Aguilar, Matias, Delgado, Nair, Court, Perles, Sahoo, Zhu, Poenisch, Flint, Sawakuchi, Beddar, Koay, Baker, Ludmir and Niedzielski. This is an open-access article distributed under the terms of the [Creative Commons Attribution License \(CC BY\)](https://creativecommons.org/licenses/by/4.0/). The use, distribution or reproduction in other forums is permitted, provided the original author(s) and the copyright owner(s) are credited and that the original publication in this journal is cited, in accordance with accepted academic practice. No use, distribution or reproduction is permitted which does not comply with these terms.

Novel pencil-beam scanning proton lattice radiation therapy for the treatment of bulky liver cancer: dosimetric comparison with VMAT-lattice radiotherapy

Yuting Li^{1,2*}, Rachael M. Martin-Paulpeter^{1,2}, Christine V. Chung¹, Miguel A. Aguilar³, Carlos A. Matias³, Adrian Delgado³, Saurabh S. Nair¹, Laurence E. Court^{1,2}, Luis Perles¹, Narayan Sahoo^{1,2}, Ronald X. Zhu¹, Falk Poenisch¹, David B. Flint^{1,2}, Gabriel O. Sawakuchi^{1,2}, Sam Beddar^{1,2}, Eugene Koay^{2,4}, Jamie S. Baker³, Ethan B. Ludmir⁴ and Joshua S. Niedzielski^{1,2*}

¹Department of Radiation Physics, The University of Texas MD Anderson Cancer Center, Houston, TX, United States, ²Graduate School of Biomedical Sciences, University of Texas Health Science Center at Houston/The University of Texas MD Anderson Cancer Center, Houston, TX, United States, ³School of Health Professions, The University of Texas MD Anderson Cancer Center, Houston, TX, United States, ⁴Department of Gastrointestinal Radiation Oncology, The University of Texas MD Anderson Cancer Center, Houston, TX, United States

Background: Spatially fractionated radiotherapy (SFRT) delivered as lattice radiotherapy (LRT) creates high-dose 'vertex' subvolumes (VTVH) embedded within low-dose 'valley' regions (VTVL) to intensify intratumoral dose while minimizing radiation dose and toxicity to organs at risk (OARs). We developed a pencil-beam scanning (PBS) intensity modulated proton therapy (IMPT) LRT planning approach and dosimetrically compared it directly with contemporary photon-based volume modulated arc therapy (VMAT) LRT for liver cancer with bulky tumors.

Methods: Twenty-one retrospective liver cases were replanned in RayStation to a single fraction of 20 Gy to VTVH with explicit VTVL sparing (mean dose <5Gy). Primary dosimetric endpoints were VTVH D80 and VTVL mean dose (analogous to mean valley dose), with secondary endpoints of VTVH/VTVL ratios (PVDR-like metrics at D80/D90/D100), VTVL D5/D80, GTV D10/D90, and planning risk volume (PRV) 0.03 cm³ hotspots. Statistical analysis consisted of paired tests (t-test or Wilcoxon signed-rank) after assessing data normality (Shapiro-Wilk tests) and using $\alpha=0.05$ for significance.

Results: Compared with photon VMAT-LRT, IMPT-LRT significantly reduced VTVL mean dose ($p<0.00001$) and increased VTVH D80 ($p<0.00001$), yielding higher VTVH/VTVL ratios at D80/D90/D100 (all $p<0.00001$). Gross tumor volume (GTV) heterogeneity (D20/D80) significantly increased with proton-LRT

($p < 0.00001$) and OAR hot-spot metrics (PRV D0.03cc) were comparable between both modalities ($p = 0.71$).

Conclusions: A robust PBS proton-LRT planning approach was developed and compared to photon VMAT-LRT for large liver tumors. Our IMPT-LRT approach maximizes peak-to-valley separation and simultaneously maintains target coverage while significantly reducing valley dose, as compared to traditional VMAT-LRT. These findings support future prospective clinical evaluation.

KEYWORDS

bulky tumor, hepatocellular carcinoma, lattice radiation therapy, liver cancer, peak-to-valley dose ratio, proton therapy, VMAT, spatially fractionated radiation therapy

Introduction

Liver cancer presents great challenge for radiation therapy (RT) due to the desired preservation of liver function, tumor proximity to critical organs, and motion uncertainties due to respiration and peristalsis; these confounding factors are further amplified when in the setting of bulky liver tumors (1–3). Radiation dose escalation is limited due to the risk of radiation-induced liver disease (RILD) and the need to spare adjacent gastrointestinal organs, which often leads to conservative dose constraints even with utilization of advanced imaging and motion management techniques during radiation delivery (1, 4). Maintaining functional hepatic reserve is a primary determinant of safety. Classic NTCP/QUANTEC analyses link mean liver dose and spared liver volume to the risk of classic RILD and contemporary guidelines for primary liver cancers recommend preserving a critical volume of uninvolved liver (e.g., $\geq 700 \text{ cm}^3$ kept below 15 Gy for 3 fractions or 21 Gy for 5 fractions in SBRT schemas) and constraining mean liver dose within 28 Gy or 32 Gy depending on the diagnosis, particularly in cirrhotic patients (1, 5, 6). These realities motivate development of radiation therapy modalities that would intensify tumor dose while maintaining mean liver dose and meeting organ-at-risk (OAR) dose constraints.

Spatial Fractionated Radiotherapy (SFRT) has re-emerged as an advanced radiation therapy approach that is particularly well-suited to treat deep-seated lesions (7). Rather than aiming for uniform target coverage, SFRT intentionally delivers a spatially modulated dose with alternating high-dose “peaks/vertices” and low-dose “valleys,” while maintaining OAR dose within tolerance. Historically, GRID, one types of SFRT, used a physical GRID block to create a 2D pattern (8); one drawback to GRID is that the 2D treatment approach is not well suited for deep-seated tumors due to rapid dose falloff as a function of depth. Subsequent advances in multi-leaf collimation and inverse planning has enabled the wide-spread adoption of lattice radiotherapy (LRT), another form of SFRT in which spherical high-dose vertices are distributed throughout the gross tumor volume (GTV) in a lattice pattern, thereby enabling advantageous dose distribution within deep-seated

tumor, such as bulky liver cancer (7, 9, 10). Current publications about LRT have established general consensus about vertex coverage, valley dose, peak-to-valley dose ratio (PVDR), and planning approaches, which has enabled the clinical translation of LRT (11, 12).

LRT is typically utilized using volume modulated arc therapy (VMAT) on standard photon-based linear accelerators and has demonstrated its capability of creating high intratumoral vertices and meeting OAR dose constraints (13, 14). However, exit dose and integral dose remain intrinsic to photons, and maintaining low valley dose becomes progressively more challenging as tumor size increases, potentially limiting the extent of dose escalation or fraction numbers achievable in the setting of photon LRT (12, 14–16).

Proton therapy offers dosimetric advantage over photon-based RT due to its sharp distal fall-off, the so-called Bragg peak, which eliminates beam exit dose, as well as overall integral dose. Given the potential immune modulating advantages of SFRT, reduction of integral dose in the tumor volume is a challenge in photon-based SFRT (17, 18). Naturally, this raises the hypothesis that proton-based LRT could significantly lower valley dose and improve PVDR-like metrics relative to photon-based LRT, particularly for large hepatic targets.

To elucidate the potential utility of proton-based LRT in the setting of bulky liver cancers, we developed a practical treatment planning strategy to implement LRT with intensity modulated proton therapy (IMPT) using a clinical pencil beam scanning (PBS) proton beam line. We also performed a paired dosimetric comparison of IMPT-LRT with photon VMAT-LRT in a retrospective cohort of liver cancer patients with bulky disease. The aim of this work was to determine if IMPT-LRT is superior in minimization of valley dose and maximization of PVDR dose characteristics, while maintaining peak vertex dose coverage, as compared to standard photon-based VMAT-LRT, under a common clinically prescribed, single-fraction 20Gy LRT treatment (11, 12, 16, 19, 20).

This work contributes three elements for the clinical SFRT community: (i) a reproducible, liver-specific IMPT-LRT planning

workflow with robust optimization; (ii) quantitative, paired evidence against a standard-of-care VMAT-LRT implementation using the same lattice geometry; and (iii) a reporting framework anchored to consensus SFRT/LRT metrics to facilitate cross-study comparison and protocol development.

Materials and methods

Study design and cohort

We performed a retrospective planning study of 21 large liver cancer cases. CT datasets and structure sets were collected from previous conventional RT clinical plans, which have been contoured and approved by the treating radiation oncologist. All 21 study patients were previously treated with breath-hold (BH) motion management technique to minimize respiratory motion during RT. For each patient, identical planning CT and structure sets were used to ensure consistency between IMPT and VMAT LRT plans. A single-fraction prescription of 20 Gy to the high-dose lattice vertices (Vertex Tumor Volume-High, VTVH) was utilized and plans were reviewed for clinical acceptability by clinical physicists and physicians.

Lattice creation and clinical goals

A script in RayStation has been developed to generate spherical prescriptive VTVH (high-dose vertices) and vertex tumor volume-low (VTVL, valley dose avoidance structure) within the radiation oncologist contoured clinical GTV. 1 cm margin was given to the edge of GTV and from OARs when constructing the lattice structures. Lattice characteristics (i.e., vertex size and spacing) conformed to a standard protocol according to GTV size. For patients with GTV <1000 cm³, 1-cm diameter spheres with 3 cm superior-inferior and 4 cm lateral center-to-center (CTC) spacing were created. For cases with GTV ≥1000 cm³, sphere diameters increased to 1.5 cm with 3-cm and 6-cm superior-inferior and lateral CTC spacing, respectively. This lattice placing strategy was established during planning study for VMAT cases, which would guarantee the optimal PVDR. Same lattice arrangement is used for each patient in VMAT and IMPT cases. Two examples of lattice construction are shown in [Figure 1](#). Planning dose constraints and objectives are listed in [Table 1](#).

VMAT-LRT planning

VMAT-LRT plans were created in our institution's clinical TPS (RayStation, RaySearch Laboratories; Stockholm, Sweden) using a 6FFF beam energy with 3–5 full arcs, multiple collimator angles (0°, 15°, 30°, and/or 90°) and a Truebeam (Varian Medical Systems; Palo Alto, CA) beam model with collapsed cone convolution dose algorithm and 2mm dose grid. Optimization objectives prioritized

VTVH coverage and VTVL sparing while meeting OAR limits. OAR constraints consisted of heart max dose <8 Gy, right kidney max dose <10Gy and PRV max dose <8 Gy. The OAR_PRV structure was defined as the concatenation of bowel, stomach, duodenum, and esophagus, plus a 5-mm expansion margin.

IMPT-LRT planning

Proton lattice plans were created with the clinical beam model for Hitachi (Hitachi Ltd. Tokyo, Japan) ProBeat proton delivery system in RayStation. PBS dose calculation was done with RayStation Monte Carlo model and 2-mm dose grid, which is the same as the corresponding VMAT plan. Hitachi ProBeat is a synchrotron based, 4-room treatment system, where proton beam with 83 discrete energies ranging from 70.2 MeV to 228.7 MeV can be generated. The same structure sets (clinical GTV, lattice ROIs, and OARs) were used for planning as the VMAT-LRT plans. The identical lattice ROIs (i.e., VTVH and VTVL) and locations were used for both VMAT-LRT and IMPT-LRT plans. For every patient, two anterior oblique and one posterior oblique beams along the vertex lines of lattice were used, and beam arrangements aimed to avoid directly opposing beams, and maximize VTVH coverage and to minimize both VTVL and OAR doses. A range shifter was not used in planning due to the non-superficial nature of lattice target structures, where the 83 discrete energies can cover the WET varying from 4cm to 32.4cm. Energies per plan were selected automatically by the optimizer based on the size and depth of the vertices, 5-mm spot spacing was used in each energy layer, and dose repainting was used to minimize the interplay effect for IMPT-LRT delivery (4). Robust optimization included 3.5% range and 3-mm setup uncertainties. A constant 1.1 RBE was used for proton plans. Robust min DVH objective was used for VTVH to achieve vertex coverage and conformity, and various robust max DVH objectives were used for VTVL to achieve dose sparing. Iterative approach was taken for each plan to achieve the desired PVDR. We have included the optimization objectives in one IMPT-SFRT plan in [Figure 2](#) for reference.

Endpoints and statistics

Primary endpoints were VTVH D80 and VTVL mean dose (analogous to mean valley dose). Secondary endpoints included, VTVH/VTVL ratios (PVDR-like metrics at D80/D90/D100), VTVL D5/D80, GTV D20/D80, and OAR_PRV 0.03 cm³ hotspots. Normality of paired differences was assessed using Shapiro–Wilk. If normality was not rejected, we used paired t-tests; otherwise, Wilcoxon signed-rank tests (two-sided, $\alpha=0.05$). For multiple endpoints, the familywise error rate was controlled via Holm adjustment; the primary endpoint is specified in the Results. We report mean \pm SD for endpoints analyzed by paired t-test and median (min–max) for those analyzed by the Wilcoxon signed-rank test; exact p-values are provided in [Tables 2–4](#).

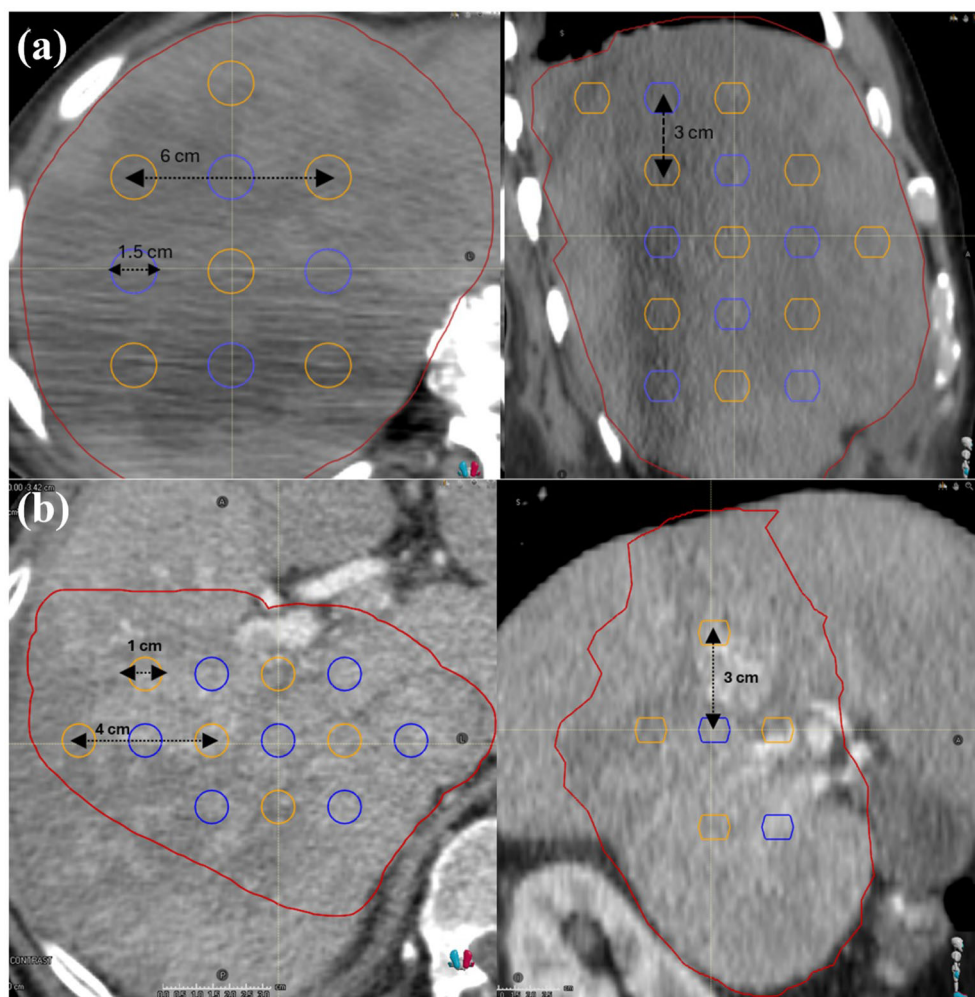


FIGURE 1 Lattice construction for tumor volume under and over 1000 cm³, where high-dose vertices (VTVH) are shown in blue, and low dose avoidance vertices (VTVL) are shown in orange. Sphere creation and layout for tumors with a gross tumor volume of (a) greater than or equal to 1000 cm³, and (b) less than 1000 cm³.

Results

VTVL (valley) sparing and VTVH (peak) coverage

A comparison of IMPT-LRT and VMAT-LRT dose distributions and dose-volume histogram (DVH) metrics for VTVL and VTVH are shown for a sample patient from the 21

patient study cohort in Figure 2. An overall trend of higher VTVH target coverage and lower VTVL valley doses is seen in IMPT-LRT plans, when compared to VMAT-LRT plans, as shown in Figure 3.

VTVL dose metrics and paired statistical analysis results are listed in Table 2. For all the 21 patients studied, IMPT-LRT achieved a consistent and statistically significant reduction in VTVL mean dose compared with VMAT-LRT (subgroup averages, 1.89 Gy vs. 3.56 Gy; p=1.41E-09). This trend of lower VTVL doses from IMPT-LRT, as compared to VMAT-LRT, was consistent for all metrics examined (i.e., VTVL D5, VTVL D50, VTVL D80, VTVL D90). Qualitatively, intratumoral low-dose corridors were better preserved between vertices for IMPT-LRT, along with reduced exit and integral dose.

VTVH dose metrics and paired statistical analysis results are listed in Table 3. Not only did IMPT-LRT plans show a significant reduction of valley dose (VTVL), but lattice target coverage (VTVH) was either consistent between both LRT approaches, or even significantly improved by IMPT-LRT for some dose metrics

TABLE 1 Planning dose constraints.

Metric	Constraints
VTVH Dmean	≥ 20 Gy
VTVH D80	≥ 20 Gy
VTVL Dmean	≤ 4 Gy
VTVL D5	≤ 5 Gy

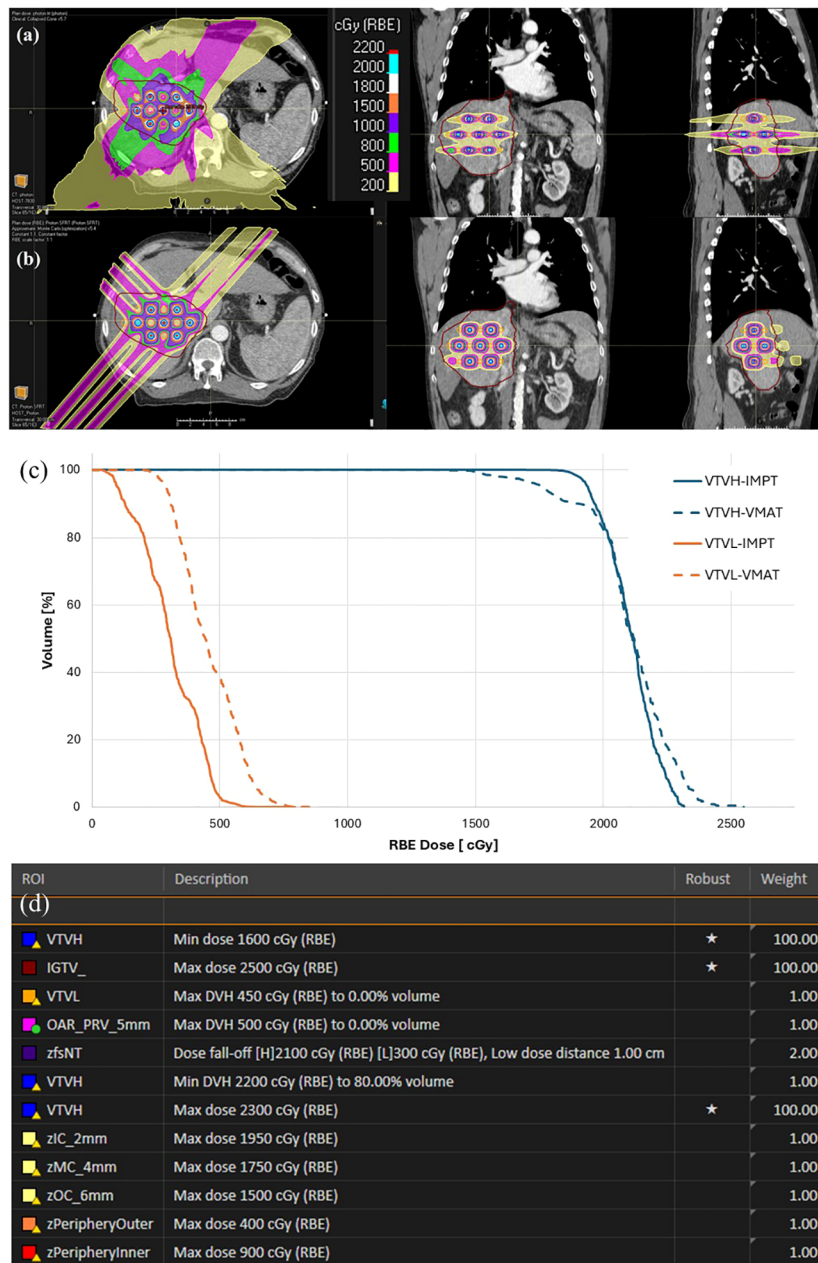


FIGURE 2 Example patient comparison of dose distributions and DVH for VMAT-LRT and IMPT-LRT. Axial, coronal, sagittal dose distributions illustrating dose distribution in (a) VMAT-LRT and (b) IMPT-LRT. (c) DVHs for VTVH and VTVL comparing VMAT-LRT and IMPT-LRT. (d) Optimization objectives used in IMPT-SFRT planning. Besides VTVH, VTVL, IGTV and fsNT, other structures are ring structures to control the dose fall off.

(i.e., VTVH D80, VTVH D90, VTVH D100; Table 3). For example, IMPT-LRT increased vertex coverage over VMAT-LRT, as measured by VTVH D80 (subgroup averages, 21.24 Gy vs. 20.37 Gy; $p=0.000024$), without compromising OAR acceptability under the same lattice design. This translated into higher VTVH/VTVL dose-ratio metrics (PVDR surrogates) at D80, D90, and D100 (all $p<0.000001$), indicating stronger peak-to-valley separation across a range of isodose percentiles for IMPT-LRT.

Global target heterogeneity

The paired statistical analysis for GTV coverage is listed in Table 4. Gross tumor dose heterogeneity (GTV D20/D80) increased with IMPT-LRT when compared to VMAT-LRT (subgroup average ratios, 55.14 vs. 5.10; $p=9.54 \times 10^{-7}$). In the lattice context, greater heterogeneity reflects more intense vertices embedded within preserved valleys, which is a desirable property when valley dose is simultaneously reduced.

TABLE 2 VTVL and PRV dose metrics and statistical comparison between VMAT-LRT and IMPT-LRT.

Dose metric	VMAT-LRT (Gy)	IMPT-LRT (Gy)	P value
Mean Dose	3.56 (2.98-4.58)	1.89 (0.81-3.04)	1.41E-09 [†]
VTVL D5	4.89 (4.05-7.47)	3.76 (2.13-4.76)	1.91E-06 [†]
VTVL D50	3.47 (2.83-4.43)	1.78 (0.56-3.03)	5.03E-07 [†]
VTVL D80	2.91 (2.28-3.45)	0.91 (0.15-2.04)	8.90E-08*
VTVL D90	2.67 (1.93-3.16)	0.58 (0.09-1.35)	2.10E-08*
VTVL D100	1.80 (1.13-2.37)	0.13 (0.01-0.44)	4.55E-11*
PRV 0.03cm ³	6.66 (3.27-10.20)	5.75 (0.02-9.59)	0.071 [†]

a) [†]Paired t-test performed; *Paired Wilcoxon rank test performed.
 b) Mean (min-max) dose.

TABLE 3 VTVH dose metrics and statistical comparison between VMAT-LRT and IMPT-LRT.

Dose metric	VMAT-LRT (Gy)	IMPT-LRT (Gy)	P value
VTVH D5	24.65 (23.52-26.02)	23.47 (22.37-24.46)	8.79E-07 [†]
VTVH D50	21.93 (21.21-22.94)	22.17 (21.14-22.88)	1.40E-05 [†]
VTVH D80	20.37 (20.00-21.34)	21.24 (20.11-22.05)	9.00E-04*
VTVH D90	19.22 (17.88-20.64)	20.69 (19.68-21.60)	0.062*
VTVH D100	10.85 (6.83-16.43)	16.32 (10.67-18.91)	2.38E-05 [†]
VTVH/VTVL D80	8.36 (5.82-33.37)	38.42 (9.86-123.47)	1.91E-06*
VTVH/VTVL D90	8.81 (6.06-37.90)	64.86 (15.07-204.60)	9.99E-08*
VTVH/VTVL D100	7.48 (3.83-33.23)	360.48 (41.57-1844)	7.25E-07*

a) [†]Paired t-test performed; *Paired Wilcoxon rank test performed.
 b) Mean (min-max) dose.

Plan acceptability and qualitative review

All plans met the single-fraction lattice goals (VTVH D80 ≥ 20 Gy, VTVL mean dose ≤ 4 Gy; VTVL D5 ≤ 5 Gy) while satisfying site-specific OAR limits during physics review. Dose displays in representative cases illustrated clearer separation between vertex peaks and valleys in IMPT-LRT, as shown in Figure 2.

Discussion

This study establishes a practical PBS IMPT-LRT planning strategy for large liver tumors and demonstrates that IMPT-LRT can simultaneously deepen valleys and strengthen vertex coverage in a paired comparison with contemporary VMAT-LRT under a

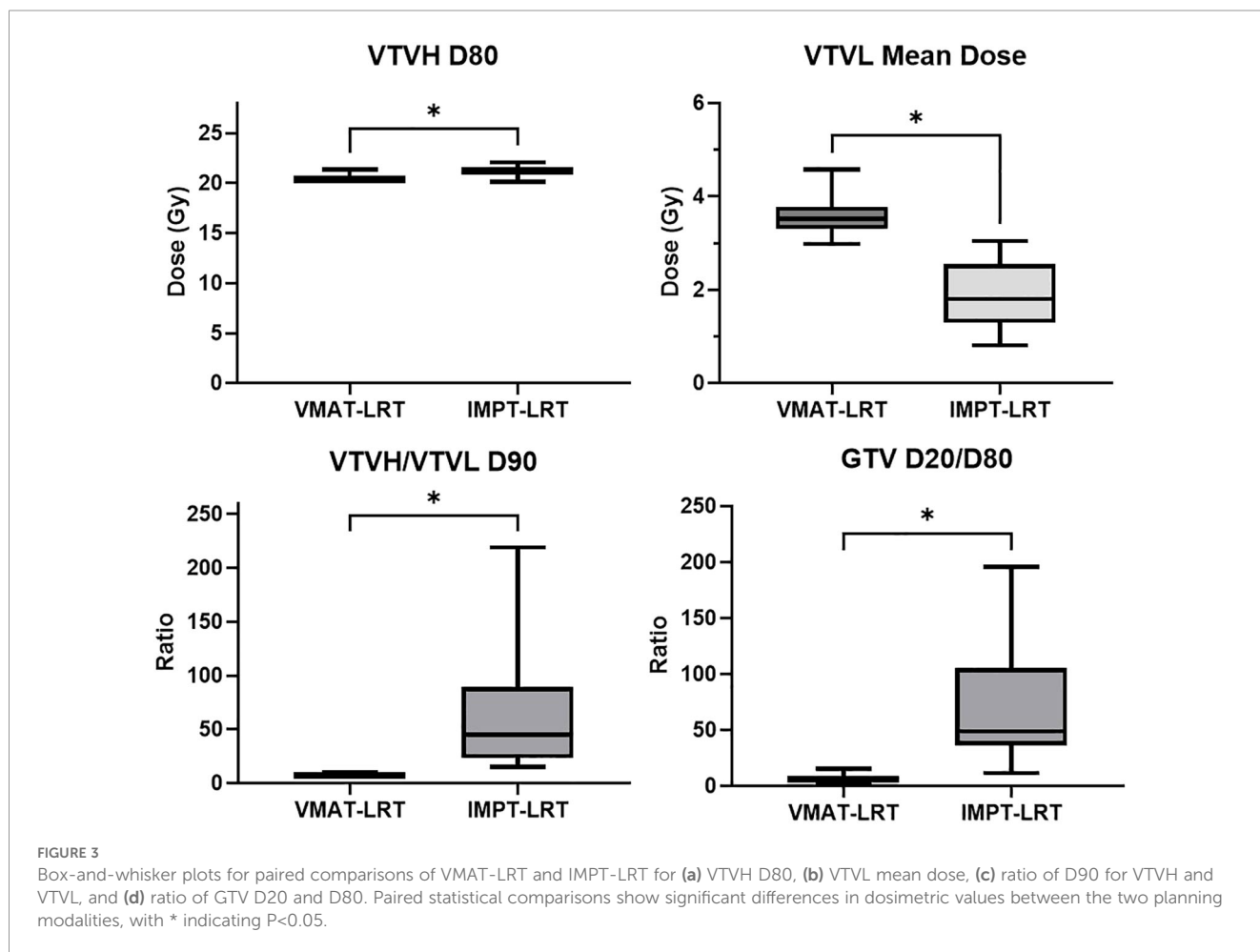


TABLE 4 GTV coverage and statistical comparison between VMAT-LRT and IMPT-LRT.

Dose metric	VMAT-LRT (Gy)	IMPT-LRT (Gy)	P value
GTV D5	10.78 (8.47-13.52)	14.08 (10.61-17.61)	3.60E-10*
GTV D10	8.05 (6.17-10.23)	9.85 (6.99-12.46)	6.92E-08*
GTV D20	5.55 (4.12-7.54)	6.00 (3.75-8.30)	0.023*
GTV D50	2.32 (1.28-3.84)	1.51 (0.32-3.46)	0.000194*
GTV D80	1.09 (0.29-2.22)	0.16 (0.03-0.63)	9.54E-07 [†]
GTV D90	0.60 (0.19-1.43)	0.06 (0.01-0.22)	9.54E-07 [†]
GTV D100	0.15 (0-0.42)	0.02 (0-0.02)	1.91E-06 [†]
GTV D20/D80	5.10 (3.40-14.21)	55.14 (303.60-946)	9.54E-07 [†]

a)[†]Paired t-test performed; *Paired Wilcoxon rank test performed.

b) Mean (min-max) dose.

single-fraction 20 Gy template. The dosimetric advantages we observed are aligned with the physical properties of protons due to its minimal exit dose and lower integral dose, and with SFRT theory that prioritizes low valley dose and robust PVDR-like metrics for therapeutic index.

While we examined proton LRT in this study, there are currently other proton SFRT modalities under investigation. Proton minibeam radiotherapy (pMBRT) had drawn attention due to its striking normal-tissue sparing in preclinical brain/skin models and early patient-specific planning studies using thick multi-slit collimators at the nozzle exit (21–24). However, pMBRT remains largely preclinical because maintaining PVDR is depth-limited and challenging for deep tumors (e.g., PVDR ≈8–12 at ~20 mm, but ≈1.1–1.6 by ~80–90 mm of depth in tissue) (25). Also, pMBRT clinical delivery either relies on mechanical collimation which reduces efficiency and adds neutron production, or requires an optimized/new nozzle since current PBS nozzles are not suitable for magnetic minibeam generation (26–31). These limitations and sensitivity to motion for sub-millimeter patterns make pMBRT less immediately deployable for deep, moving abdominal targets like the liver (4, 24). In contrast, our PBS-based IMPT-LRT strategy is directly analogous to photon LRT (with growing clinical experience), uses standard hardware and TPS, integrates with robust optimization for motion/range, and is therefore more clinically applicable in the near term.

From a translational perspective, enhanced vertex and valley dose ratio and lower liver dose, support several clinical pathways: (i) single-fraction IMPT-LRT as a boost preceding or following conventionally fractionated EBRT; (ii) multi-fraction IMPT-LRT (e.g., 3–5 fractions) to balance biologic effectiveness and OAR recovery; and (iii) selective dose escalation for very large GTVs where photon lattice plans struggle to keep mean liver dose and central hepatobiliary tract within dose constraints. These strategies are consistent with emerging SFRT consensus documents and proton LRT planning reports emphasizing standardized vertex/valley endpoints (VTVH D80, VTVLmean, PVDR-like ratios) and robust delivery practices (range/setup robustness, gating/DIBH, repainting).

Our work focused on bulky liver cancer due to the complexity of treating this disease, as well as recent clinical results with liver LRT that show it is an emerging treatment approach. A 2023 systematic review concluded that LRT appears safe, with heterogeneous but promising efficacy signals across multiple treatment sites, while emphasizing the need for standardized endpoints and prospective data specific to the liver (32). For hepatocellular carcinoma (HCC), dosimetric feasibility work shows that VMAT-LRT can escalate intratumoral dose when conventional SBRT is OAR-limited, supporting the rationale for spatially modulated boosts in challenging hepatic presentations (8, 33). Clinically, a recent liver-focused case demonstrated rapid palliation and marked volumetric response after single-fraction 16 Gy LRT delivered to ~1% of the metastatic liver burden while keeping the mean liver dose ≈3 Gy and without acute toxicity, highlighting the potential of LRT to relieve symptoms at very low integral dose (15). Considering these circumstances, our PBS proton LRT workflow is designed to enhance valley sparing and lower non-target liver dose relative to VMAT-LRT, which should lead to better protection of functional parenchyma and facilitate dose intensification or fraction reduction in large hepatic targets. Mechanistically, improved valley sparing may better protect functional liver parenchyma, potentially lowering the risk of RILD when combined with following EBRT (1, 5, 34). At the same time, higher vertex doses could enhance intratumoral cytotoxicity and immune priming in heterogeneous hypoxic tumors (35–37). Our findings therefore provide a dosimetric foundation for protocol development in hepatic SFRT/LRT that prospectively measures liver function (e.g., ICG, HIDA, or SPECT/PET) alongside clinical toxicity and local control.

Delivery considerations are paramount for the liver. Proton PBS delivery is more sensitive to interplay effect due to respiration and peristalsis motions, and proton range uncertainty comparing with photon modalities. As a result, proper planning approaches and motion management strategies need to be established for IMPT-LRT to mitigate setup uncertainties, anatomical variations (from intra- and inter-fractional motion), and range uncertainties. In this study, inspiration breath hold gating was used during initial simulation for the patients included in this study. During planning, a 3-mm setup and 3.5% range uncertainty parameters were used in robust optimization, which is consistent with our clinical stereotactic body radiation therapy treatments that utilize protons. The 3mm setup uncertainty takes into account of patient setup variation and spot positioning accuracy. For liver stereotactic treatment, CT-on-Rails (CTOR) which has superior imaging quality than CBCT will be used during patient setup to minimize the setup error. Spot position accuracy is checked daily and monitored by the ProBeat system during treatment, where an averaged 1mm accuracy is expected. Before implementing in clinic, End-to-end tests will be conducted to evaluate the efficiency of the 3mm setup uncertainty.

This study had several limitations. First, this study used a planning-only study design (lack of delivery QA). The vertex integrity and valley sparing could be compromised during treatment due to variation of spot positioning, range uncertainties, patient's position variations. End-to-end tests would be needed to establish the

treatment protocol. Second, we used a relative biological effectiveness (RBE) factor of 1.1 for proton therapy, which may not sufficiently capture high-dose-per-fraction biology. We did not perform organ-specific statistical testing or subgroup analyses by GTV size. Nevertheless, the consistency of valley sparing across all cases and the magnitude of the PVDR-like improvements support the generalizability of the core finding. The second limitation is lack of strategy for robustness evaluation. During our clinical implementation of IMPT SFRT, for each candidate plan we will compute robustness scenarios including standard setup and range uncertainties and, critically, motion-specific scenarios, then assess three SFRT metrics per scenario: peak coverage within VTVH (e.g., D95), valley dose in the valley volume adjacent to the relevant OAR interface, and the resulting PVDR. For free-breathing deliveries, robustness will explicitly evaluate dose calculated on scans of T0 and T50; for DIBH, we will propagate the plan across multiple repeat breath-hold CTs acquired at simulation to capture breath-hold variability. We will summarize results as both scenario-average and scenario-minimum (“worst-case”) values, and reported as PVDR_robust, peak-coverage robust, and valley-dose robust, and require that all meet predefined acceptance thresholds, with particular emphasis on preserving PVDR_robust at the tumor-OAR interface. When thresholds are not met, we will iterate geometry and delivery (vertex size/placement, repainting, gating/beam timing, or modest beam re-arrangement). The third limitation is that this study only focuses on liver tumors. We focus on bulky liver tumors because (i) hepatic toxicity tightly correlates with the volume of uninvolved liver receiving low-intermediate dose, making valley sparing particularly impactful; (ii) tumors often in close proximity to stomach/duodenum/bile ducts, where sharper dose fall-off may reduce OAR toxicities; (iii) the liver’s respiratory motion is manageable with 4D robust optimization, gating/repainting, fiducial/surface guidance or breath-hold techniques; and (iv) liver IGRT is mature yet imperfect, so range-modulated valleys may better protect parenchyma under uncertainty. This setting offers a clean readout of proton IMPT LRT’s dosimetric advantage. Future work will evaluate proton IMPT LRT in additional sites and histologies that photon LRT has shown feasibility and early clinical signal, which includes non-small cell lung cancer (NSCLC), head and neck, gynecologic (bulky cervix), and soft-tissue sarcoma. In voluminous NSCLC, retrospective data suggest safety and tumor response (38). Palliative head-and-neck series report symptom relief with acceptable toxicity (39). Prospective multi-site data (LITE SABR M1) support short-term safety in large tumors, and time-resolved case series show rapid palliation across sites (40, 41). For gynecologic disease, far-advanced cervical cancer has demonstrated high metabolic responses with good tolerance after LRT (42). In sarcoma, neoadjuvant extremity cases show technical feasibility of integrating high-dose lattice with standard RT (43). These experiences motivate site-specific proton LRT protocols to test whether enhanced valley-sparing can further reduce normal-tissue dose while preserving (or improving) clinical benefit.

Future work will include LET optimization to further enhance the dose contrast in vertex and valley, and thorough study of organ-

specific studies for different lattice construction and different planning techniques, as well as understanding the RBE effects of proton LRT in clinical treatment planning and delivery.

Moreover, only DIBH was used as motion management method in this planning study. Based on our experience in proton treatment, respiratory excursions over 5 mm produce phase-dependent hot/cold spots between T0 (end-inspiration) and T50. This effect would amplify and erode planned PVDR in single-fraction SFRT, where minimal temporal averaging leaves interplay unmitigated. We therefore will explore a threshold-based policy for future study: for motion less than 5mm, we create the plan using free breathing CT scan with T0/T50 explicitly included in robust optimization and apply layered repainting during delivery. For motion equal to or higher than 5mm, we treat with deep-inspiration breath-hold (DIBH) and, to account for breath-hold variability between simulation and treatment, acquire more than 3 repeat DIBH CTs at simulation and include all repeats in robustness optimization. If DIBH proves infeasible, we revert to amplitude/phase gating with compression and increase repainting to further mitigate interplay (44, 45). As a future direction, we will prospectively benchmark PVDR erosion vs motion amplitude, test whether multi-CT DIBH planning stabilizes valley dose relative to single-CT approaches, and define adaptive re-simulation triggers (e.g., >2–3 mm drift in observed motion or breath-hold level). Recent developments in proton SFRT include robust multi-field planning strategies (e.g., primary plus robust complementary beams) and proton arc-based lattice (ARC/SPArc) are concepts that seek to balance vertex intensification with valley suppression and OAR sparing (19, 20, 30). Motion management strategies and planning studies could be explored with proton ARC/SPArc lattice concepts to further reduce the valley dose and minimize entrance dose, albeit at the slight increase of integral dose.

Conclusion

In summary, proton-based IMPT-LRT is feasible and shows significant dosimetric advantages over traditional photon-based VMAT-LRT for liver tumors in this paired planning study. IMPT-LRT provided superior valley sparing and higher vertex coverage than VMAT-LRT for large liver tumors, with comparable PRV hotspots under a shared lattice template. In terms of plan quality and dosimetry, our results establish IMPT-LRT as a superior modality to VMAT-based LRT with deeper valleys, stronger peaks, same OAR safety, and provide a quantitative basis for prospective clinical implementation (e.g., boost strategies or multi-fraction LRT).

Data availability statement

The raw data supporting the conclusions of this article will be made available by the authors, without undue reservation.

Ethics statement

The studies involving humans were approved by University of Texas MD Anderson Cancer Center IRB. The studies were conducted in accordance with the local legislation and institutional requirements. Written informed consent for participation was not required from the participants or the participants' legal guardians/next of kin in accordance with the national legislation and institutional requirements.

Author contributions

YL: Writing – original draft, Formal analysis, Writing – review & editing, Data curation, Validation. RM-P: Data curation, Writing – review & editing, Writing – original draft, Investigation. CC: Writing – original draft, Methodology, Investigation, Data curation, Writing – review & editing. MA: Writing – original draft, Investigation, Writing – review & editing, Formal analysis, Data curation. CM: Data curation, Writing – review & editing, Investigation, Writing – original draft, Formal analysis. AD: Formal analysis, Data curation, Writing – review & editing, Investigation, Writing – original draft. SN: Writing – review & editing, Writing – original draft. LC: Writing – review & editing, Writing – original draft. LP: Methodology, Writing – review & editing, Investigation, Writing – original draft. NS: Writing – original draft, Writing – review & editing. RZ: Writing – original draft, Writing – review & editing. FP: Writing – original draft, Methodology, Investigation, Writing – review & editing. DF: Writing – review & editing, Writing – original draft, Investigation. GS: Writing – review & editing, Writing – original draft, Methodology. SB: Writing – review & editing, Writing – original draft, Methodology. EK: Writing – original draft, Writing – review & editing. JB: Investigation, Writing – original draft, Writing – review & editing. EL: Methodology, Writing – review & editing, Writing – original draft. JN: Writing – review & editing, Formal analysis, Data curation, Project administration, Methodology, Validation, Investigation, Supervision, Conceptualization, Writing – original draft.

References

1. Apisarnthanarax S, Barry A, Cao M, Czit Bo, DeMatteo R, Drinane M, et al. External beam radiation therapy for primary liver cancers: an ASTRO clinical practice guideline. *Pract Radiat Oncol.* (2022) 12:28–51. doi: 10.1016/j.prro.2021.09.004
2. Koay EJ, Owen D, Das P. Radiation-induced liver disease and modern radiotherapy. *Semin Radiat Oncol.* (2018) 28:321–31. doi: 10.1016/j.semradonc.2018.06.007
3. Singal AG, Llovet JM, Yarchoan M, Mehta N, Heimbach JK, Dawson LA, et al. AASLD Practice Guidance on prevention, diagnosis, and treatment of hepatocellular carcinoma. *Hepatology.* (2023) 78:1922–65. doi: 10.1097/HEP.0000000000000466
4. Li H, Dong L, Bert C, Chang J, Flampouri S, Jee KW, et al. AAPM Task Group Report 290: Respiratory motion management for particle therapy. *Med Phys.* (2022) 49:e50–81. doi: 10.1002/mp.15470
5. Miften M, Vinogradskiy Y, Moiseenko V, Grimm J, Yorke E, Jackson A, et al. Radiation dose and volume effects for liver SBRT. *Int J Radiat Oncol Biol Phys.* (2021) 110:196–205. doi: 10.1016/j.ijrobp.2017.12.290
6. Dawson LA, Normolle D, Balter JM, McGinn CJ, Lawrence TS, Ten Haken RK, et al. Analysis of radiation-induced liver disease using the Lyman NTCP model. *Int J Radiat Oncol Biol Phys.* (2002) 53:810–21. doi: 10.1016/S0360-3016(02)02846-8
7. Zhang H, Wu X, Zhang X, Chang SX, Megooni A, Donnelly ED, et al. Photon GRID radiation therapy: A physics and dosimetry white paper from the radiosurgery society (RSS) GRID/LATTICE, microbeam and FLASH radiotherapy working group. *Radiat Res.* (2020) 194:665–77. doi: 10.1667/RADE-20-00047.1
8. Mohiuddin M, Curtis DL, Grizos WT, Komarnicky L. Palliative treatment of advanced cancer using multiple nonconfluent pencil beam radiation. *A Pilot Study*

Funding

The author(s) declared financial support was received for this work and/or its publication. JSN reports funding from the National Institutes of Health (NHLBI 1K23HL175243-01A1 and NCI 1L30CA305700-01).

Acknowledgments

We thank the clinical physics and dosimetry teams at the University of Texas MD Anderson Cancer Center for plan review and discussions.

Conflict of interest

The authors declared that this work was conducted in the absence of any commercial or financial relationships that could be construed as a potential conflict of interest.

Generative AI statement

The author(s) declared that generative AI was not used in the creation of this manuscript.

Any alternative text (alt text) provided alongside figures in this article has been generated by Frontiers with the support of artificial intelligence and reasonable efforts have been made to ensure accuracy, including review by the authors wherever possible. If you identify any issues, please contact us.

Publisher's note

All claims expressed in this article are solely those of the authors and do not necessarily represent those of their affiliated organizations, or those of the publisher, the editors and the reviewers. Any product that may be evaluated in this article, or claim that may be made by its manufacturer, is not guaranteed or endorsed by the publisher.

- Cancer*. (1990) 66:114–8. doi: 10.1002/1097-0142(19900701)66:1<114::AID-CNCR2820660121>3.0.CO;2-L
9. Setianegara J, Zhu YN, Zhu M, Badkul R, Zhao T, Li H, et al. Proton GRID and LATTICE treatment planning techniques for clinical liver SFRT treatments. *Phys Med Biol*. (2025) 70. doi: 10.1088/1361-6560/add2cc
10. Wu X, Ahmed MM, Wright J, Gupta S, Pollack A. On modern technical approaches of three-dimensional high-dose lattice radiotherapy (LRT). *Cureus*. (2010) 2:e9. doi: 10.7759/cureus.9
11. Li H, Mayr NA, Griffin RJ, Zhang H, Pokhrel D, Grams M, et al. Overview and recommendations for prospective multi-institutional spatially fractionated radiation therapy clinical trials. *Int J Radiat Oncol Biol Phys*. (2024) 119:737–49. doi: 10.1016/j.ijrobp.2023.12.013
12. Mayr NA, Snider JW, Regine WF, Mohiuddin M, Hippe DS, Peñagaricano J, et al. An international consensus on the design of prospective clinical-translational trials in spatially fractionated radiation therapy. *Adv Radiat Oncol*. (2022) 7:100866. doi: 10.1016/j.adro.2021.100866
13. Grams MP, Owen D, Park SS, Petersen IA, Haddock MG, Jeans EB, et al. VMAT grid therapy: A widely applicable planning approach. *Pract Radiat Oncol*. (2021) 11:e339–47. doi: 10.1016/j.prro.2020.10.007
14. Np J, Rao S, Singh A, Velu U, Mehta A, Lewis S, et al. Feasibility planning study of lattice radiotherapy for palliation in bulky tumors. *Precis Radiat Oncol*. (2024) 8:209–17. doi: 10.1002/pro6.1248
15. El Chammah S, Bendahman M, Ghandour S, Fuchs L, Kinj R, Guyer G, et al. Lattice radiotherapy for extensive liver metastases in synchronous EGFR-mutant lung adenocarcinoma and small cell lung cancer. *Clin Transl Radiat Oncol*. (2025) 54:101023. doi: 10.1016/j.ctro.2025.101023
16. Grams MP, Tseung H, Ito S, Zhang Y, Owen D, Park SS, et al. A dosimetric comparison of lattice, brass, and proton grid therapy treatment plans. *Pract Radiat Oncol*. (2022) 12:e442–52. doi: 10.1016/j.prro.2022.03.005
17. Chang MC, Chen YL, Lin HW, Chiang YC, Chang CF, Hsieh SF, et al. Irradiation enhances abscopal anti-tumor effects of antigen-specific immunotherapy through regulating tumor microenvironment. *Mol Ther*. (2018) 26:404–19. doi: 10.1016/j.ymthe.2017.11.011
18. Johnsrud AJ, Jenkins SV, Jamshidi-Parsian A, Quick CM, Galhardo EP, Dings RPM, et al. Evidence for early stage anti-tumor immunity elicited by spatially fractionated radiotherapy-immunotherapy combinations. *Radiat Res*. (2020) 194:688–97. doi: 10.1667/RADE-20-00065.1
19. Mossahebi S, Molitoris JK, Poirier Y, Jatzak J, Zhang B, Mohindra P, et al. Clinical implementation and dosimetric evaluation of a robust proton lattice planning strategy using primary and robust complementary beams. *Int J Radiat Oncol Biol Phys*. (2024) 120:1149–58. doi: 10.1016/j.ijrobp.2024.06.009
20. Zhu YN, Zhang W, Setianegara J, Lin Y, Traneus E, Long Y, et al. Proton ARC based LATTICE radiation therapy: feasibility study, energy layer optimization and LET optimization. *Phys Med Biol*. (2024) 69. doi: 10.1088/1361-6560/ad8855
21. Datzmann G, Sammer M, Girst S, Mayerhofer M, Dollinger G, Reindl J, et al. Preclinical challenges in proton minibeam radiotherapy: physics and biomedical aspects. *Front Phys*. (2020) 8. doi: 10.3389/fphy.2020.568206
22. Ortiz R, De Marzi L, Prezado Y. Proton minibeam radiation therapy and arc therapy: proof of concept of a winning alliance. *Cancers (Basel)*. (2021) 14. doi: 10.3390/cancers14010116
23. Tobola-Galus A, Swakon J, Olko P. DOSIMETRIC CHARACTERIZATION OF COLLIMATORS FOR SPATIALLY FRACTIONATED PROTON THERAPY OF THE EYE. *Radiat Prot Dosim*. (2018) 180:351–4. doi: 10.1093/rpd/ncy015
24. Yang F, Wu J, Orlandini LC, Li H, Wang X. Proton minibeam radiotherapy: a review. *Front Oncol*. (2025) 15:1580513. doi: 10.3389/fonc.2025.1580513
25. Lansonneur P, Mammar H, Nauraye C, Patriarca A, Hierso E, Dendale R, et al. First proton minibeam radiation therapy treatment plan evaluation. *Sci Rep*. (2020) 10:7025. doi: 10.1038/s41598-020-63975-9
26. De Marzi L, Patriarca A, Nauraye C, Hierso E, Dendale R, Guardiola C, et al. Implementation of planar proton minibeam radiation therapy using a pencil beam scanning system: A proof of concept study. *Med Phys*. (2018) 45:5305–16. doi: 10.1002/mp.13209
27. Dilmanian FA, Venkatesulu BP, Sahoo N, Wu X, Nassimi JR, Herchko S, et al. Proton minibeam-a springboard for physics, biology and clinical creativity. *Br J Radiol*. (2020) 93:20190332. doi: 10.1259/bjr.20190332
28. Gao M, Mohiuddin MM, Hartsell WF, Pankuch M. Spatially fractionated (GRID) radiation therapy using proton pencil beam scanning (PBS): Feasibility study and clinical implementation. *Med Phys*. (2018) 45:1645–53. doi: 10.1002/mp.12807
29. Guardiola C, Peucelle C, Prezado Y. Optimization of the mechanical collimation for minibeam generation in proton minibeam radiation therapy. *Med Phys*. (2017) 44:1470–8. doi: 10.1002/mp.12131
30. Lee JS, Mumaw DA, Liu P, Loving BA, Sebastian E, Cong X, et al. Rotationally intensified proton lattice: A novel lattice technique using spot-scanning proton arc therapy. *Adv Radiat Oncol*. (2024) 9. doi: 10.1016/j.adro.2024.101632
31. Schneider T, De Marzi L, Patriarca A, Prezado Y. Advancing proton minibeam radiation therapy: magnetically focussed proton minibeam at a clinical centre. *Sci Rep*. (2020) 10:1384. doi: 10.1038/s41598-020-58052-0
32. Iori F, Cappelli A, D'Angelo E, Cozzi S, Ghersi SF, De Felice F, et al. Lattice Radiation Therapy in clinical practice: A systematic review. *Clin Transl Radiat Oncol*. (2023) 39:100569. doi: 10.1016/j.ctro.2022.100569
33. Frankart AJ, Nelson B, Kumar N, Takiar V. Intratumoral dose escalation using lattice radiotherapy for hepatocellular carcinoma with unfavorable size and location. *Int J Radiat Oncol Biol Phys*. (2023) 117:e296. doi: 10.1016/j.ijrobp.2023.06.2306
34. Pan CC, Kavanagh BD, Dawson LA, Li XA, Das SK, Miften M, et al. Radiation-associated liver injury. *Int J Radiat Oncol Biol Phys*. (2010) 76:S94–100. doi: 10.1016/j.ijrobp.2009.06.092
35. Bekker RA, Obertopp N, Redler G, Penagaricano J, Caudell JJ, Yamoah K, et al. Spatially fractionated GRID radiation potentiates immune-mediated tumor control. *Radiat Oncol*. (2024) 19:121. doi: 10.1186/s13014-024-02514-6
36. Lukas L, Zhang H, Cheng K, Epstein A. Immune priming with spatially fractionated radiation therapy. *Curr Oncol Rep*. (2023) 25:1483–96. doi: 10.1007/s11912-023-01473-7
37. McMillan MT, Khan AJ, Powell SN, Humm J, Deasy JO, Haimovitz-Friedman A, et al. Spatially fractionated radiotherapy in the era of immunotherapy. *Semin Radiat Oncol*. (2024) 34:276–83. doi: 10.1016/j.semradonc.2024.04.002
38. Amendola BE, Perez NC, Wu X, Amendola MA, Qureshi IZ. Safety and efficacy of lattice radiotherapy in voluminous non-small cell lung cancer. *Cureus*. (2019) 11:e4263. doi: 10.7759/cureus.4263
39. Xu P, Wang S, Zhou J, Yuan K, Wang X, Li L, et al. Spatially fractionated radiotherapy (Lattice SFRT) in the palliative treatment of locally advanced bulky unresectable head and neck cancer. *Clin Transl Radiat Oncol*. (2024) 48:100830. doi: 10.1016/j.ctro.2024.100830
40. Duriseti S, Kavanaugh JA, Szymanski J, Huang Y, Basarabescu F, Chaudhuri A, et al. LITE SABR M1: A phase I trial of Lattice stereotactic body radiotherapy for large tumors. *Radiother Oncol*. (2022) 167:317–22. doi: 10.1016/j.radonc.2021.11.023
41. Studer G, Jeller D, Streller T, Huebner D, Glanzmann C. Time-related outcome following palliative spatially fractionated stereotactic radiation therapy (Lattice) of large tumors - A case series. *Adv Radiat Oncol*. (2024) 9:101566. doi: 10.1016/j.adro.2024.101566
42. Amendola BE, Perez NC, Mayr NA, Wu X, Amendola M. Spatially fractionated radiation therapy using lattice radiation in far-advanced bulky cervical cancer: A clinical and molecular imaging and outcome study. *Radiat Res*. (2020) 194:724–36. doi: 10.1667/RADE-20-00038.1
43. Hatoum GF, Temple HT, Garcia SA, Zheng Y, Kfoury F, Kinley J, et al. Neoadjuvant radiation therapy with interdigitated high-dose LRT for voluminous high-grade soft-tissue sarcoma. *Cancer Manag Res*. (2023) 15:113–22. doi: 10.2147/CMARS393934
44. Koh WYC, Tan HQ, Lew KS, Kor WTA, Samsuri NAB, Chan JWS, et al. Real-time gated proton therapy: Introducing clinical workflow and failure modes and effects analysis (FMEA). *Tech Innov Pat Support Radiat Oncol*. (2025) 34:100311. doi: 10.1016/j.tipsro.2025.100311
45. Pfeiler T, Ahmad Khalil D, Ayadi M, Bäumer C, Blanck O, Chan M, et al. Motion effects in proton treatments of hepatocellular carcinoma-4D robustly optimised pencil beam scanning plans versus double scattering plans. *Phys Med Biol*. (2018) 63:235006. doi: 10.1088/1361-6560/aacfc